THE JOURNAL OF BIOLOGICAL CHEMISTRY VOL. 286, NO. 1, pp. 35–41, January 7, 2011

Sodium Overload and Water Influx Activate the NALP3 Inflammasome[S]

Received for publication, April 28, 2010, and in revised form, October 1, 2010 Published, JBC Papers in Press, November 4, 2010, DOI 10.1074/jbc.M110.139048

Christine Schorn[‡1,2], Benjamin Frey[§3], Kirsten Lauber[¶], Christina Janko[‡2], Moritz Strysio[‡], Hildegard Keppeler[‖], Udo S. Gaipl[§3], Reinhard E. Voll[‡], Eva Springer[**], Luis E. Munoz[‡4], Georg Schett[‡], and Martin Herrmann[‡5]

From the Departments of [‡]Internal Medicine 3, [§]Radiation Oncology, and [**]Materials Science–Glass and Ceramics, the University of Erlangen-Nuremberg, 91054 Erlangen, the [¶]Department of Radiation Oncology, the University of Munich, 81377 Munich, and the [‖]Department of Internal Medicine I, University of Tuebingen, 72076 Tuebingen, Germany

The NALP3 inflammasome is activated by low intracellular potassium concentrations $[K^+]_i$, leading to the secretion of the proinflammatory cytokine IL-1β. However, the mechanism of $[K^+]_i$ lowering after phagocytosis of monosodium urate crystals is still elusive. Here, we propose that endosomes containing monosodium urate crystals fuse with acidic lysosomes. The low pH in the phagolysosome causes a massive release of sodium and raises the intracellular osmolarity. This process is balanced by passive water influx through aquaporins leading to cell swelling. This process dilutes $[K^+]_i$ to values below the threshold of 90 mM known to activate NALP3 inflammasomes without net loss of cytoplasmic potassium ions. *In vitro*, the inhibitors of lysosomal acidification (ammonium chloride, chloroquine) and of aquaporins (mercury chloride, phloretin) all significantly decreased the production of IL-1β. *In vivo*, only the pharmacological inhibitor of lysosome acidification chloroquine could be used which again significantly reduced the IL-1β production. As a translational aspect one may consider the use of chloroquine for the anti-inflammatory treatment of refractory gout.

Gout is a relapsing painful arthritis affecting 1% of the population in the industrialized countries (1). Already 2000 years ago A. C. Celsus assumed a link to an urinary solute (2). Deposition of monosodium urate crystals (MSU)[6] within joints and periarticular tissues causes massive inflammation (3). The latter is in part mediated by immune activating "danger signals." Besides ATP and HMGB1, uric acid released from dying cells has been described as such a signal (4). Martinon and colleagues showed that MSU engages the NALP3/cryopyrin inflammasome, resulting in caspase-1 activation and consecutively in the cleavage of the pro-forms of the inflammatory cytokines interleukin (IL)-1β and IL-18. The importance of the inflammasome in the etiopathogenesis of MSU-induced inflammation is highlighted by the fact that in mice deficient for either the inflammasome or the receptor for IL-1β (IL-1R) neutrophil influx is strongly reduced in crystal-induced peritonitis (5). Inflammasomes are cytoplasmic protein complexes containing caspase-1 and NOD-like receptor, which are able to activate IL-1β and IL-18 (6). The NALP3 inflammasomes are triggered by a plethora of microbial and host-derived danger-associated components, including MSU crystals (7). The common denominator of all known activators of the NALP3 and NALP1 inflammasomes is the fact that they cause a drop of the intracellular potassium concentration $[K^+]_i$ to levels below 90 mM, a milieu in which caspase-1 recruitment and inflammasome activation occurs spontaneously. This mechanism has been molecularly delineated for many inflammasome activators including pore-forming bacterial toxins (*e.g.* nigericin, aerolysin, gramicidin), activators of potassium ion channels (*e.g.* P2X7-receptor and ATP), or inhibitors of the Na^+/K^+-ATPase (ouabain). However, the mechanism engaged by MSU crystals to lower intracellular potassium is still elusive. The large-conductance Ca^{2+}-activated K^+ channel MaxiK was suggested to mediate MSU-induced inflammasome activation; however, its inhibition with paxilline did not abrogate caspase-1 activation (8). Here, we describe a novel mechanism for lowering $[K^+]_i$ and consecutive inflammasome activation after phagocytosis of MSU crystals.

EXPERIMENTAL PROCEDURES

Materials

Heparinized venous blood was obtained from several healthy donors in full agreement with institutional guidelines. Peripheral blood mononuclear cells and polymorphonuclear neutrophils (PMNs) were isolated from heparinized blood using density-gradient centrifugation following standard protocols (9). Untouched monocytes were isolated by a Monocyte Isolation Kit II from Miltenyi. Autologous plasma was extracted from heparinized venous blood by centrifugation at 3400 relative centrifugal force for 10 min. C57/BL6 mice were

[S] The on-line version of this article (available at http://www.jbc.org) contains supplemental Figs. 1–9 and Video 1.

[1] Supported by Deutsche Forschungsgemeinschaft Grant GK SFB 643, the Interdisciplinary Center of Clinical Research (IZKF) at the University Hospital of the University of Erlangen-Nuremberg and by Erlanger Leistungsbezogene Anschubfinanzierung und Nachwuchsförderung (ELAN) Fond 09.10.15.1 of the University Clinic of Erlangen.

[2] Supported by K. und R. Wucherpfennigstiftung.

[3] Supported by the Doktor Robert Pfleger Foundation and by the German Research Foundation Grant GA 1507/1-1.

[4] Supported by Erlanger Leistungsbezogene Anschubfinanzierung und Nachwuchsförderung (ELAN) Fond 09.03.18.1 of the University Clinic of Erlangen.

[5] To whom correspondence should be addressed: Dept. of Internal Medicine 3 and Institute for Clinical Immunology, University of Erlangen-Nuremberg, Krankenhausstr. 12, 91054 Erlangen, Germany. Tel.: 49 9131 85 36990; Fax: 49 9131 85 35776; E-mail: Martin.Herrmann@uk-erlangen.de.

[6] The abbreviations used are: MSU, monosodium urate; AQP, aquaporin; CQ, chloroquine diphosphate salt; $[K^+]_i$, intracellular potassium concentration; LY, Lucifer yellow; MPU, monopotassium urate; $[Na^+]_i$, intracellular sodium concentration; PI, propidium iodide; PMN, polymorphonuclear neutrophil.

purchased from Charles River Laboratories Inc. Throughout the studies, all mice were provided a special diet and water *ad libitum* and were kept individually in well ventilated cages under standard conditions of humidity (55 ± 5%), temperature (22 ± 2 °C), and light (12/12 h light-dark cycles). The animal studies were approved by the "Regierung von Mittelfranken" and conducted according to guidelines of the Federation of European Laboratory Animal Science Associations (FELASA) and the "Gesellschaft fuer Versuchstierkunde" (GV-SOLAS). This provided the assurance that the animal studies adhered to internationally accepted standards for the ethical use of animals in research. THP-1 cells (from American Type Culture Collection) were cultured in RPMI 1640 medium (10% heat-inactivated FCS, 100 units/ml penicillin, 0.1 mg/ml streptomycin, and 10 mM HEPES, all from Invitrogen). Cells were grown at 37 °C in a 5% CO_2 incubator. Human IL-1β, IL-6, and TNFα production were measured by multiplex bead array technology (Bender MedSystems). Murine IL-1β production was determined by enzyme-linked immunosorbent assay (ELISA; R&D Systems). Phorbol myristate acetate, propidium iodide (PI), chloroquine diphosphate salt (CQ), and phloretin were ordered from Sigma-Aldrich. Lucifer yellow (LY) and Sodium Green tetraacetate were from Invitrogen. Anti-CD14-PE antibody was obtained from Beckman Coulter; anti-murine CD11b antibody was from BD Pharmingen. Anti-human proIL-1β antibody was purchased from Cell Signaling; murine anti-proIL-1β, anti-rabbit-, anti-mouse-, and anti-rat secondary antibodies were from R&D Systems; human and murine anti-caspase-1 antibodies were from Santa Cruz Biotechnology. Uric acid, NaCl, KCl, NH_4Cl, and $HgCl_2$ were purchased from Merck.

For the production of MSU crystals and monopotassium urate crystals (MPU), standard protocols were used (10). A solution of 10 mM uric acid and 154 mM NaCl or 154 mM KCl, respectively, was adjusted to pH 7.2 and agitated for 3 days at 37 °C. The crystals were baked for 2 h at 180 °C to remove potentially contaminating LPS.

Methods

Morphological Analysis of Phagocytes after MSU Uptake—Whole blood cells were stained with an anti-CD14-PE antibody for identification of monocytes. After that, 1 mg/ml MSU crystals were added and incubated at 37 °C for 1 h. The ingestion of MSU crystals was determined by flow cytometry. The uptake of MSU crystals was reflected by an increased side scatter of phagocytes.

Determination of Membrane Integrity by PI—Whole blood cells were treated with 1 mg/ml MSU and stained with 3 μg/ml membrane-impermeable fluorescent dye PI. If the cell membrane loses its membrane integrity, PI forms a fluorescent complex with nuclear DNA (11). After 3 h, noningested crystals were solubilized, and cells were analyzed by flow cytometry. Heat-necrotized cells (30 min, 56 °C) served as controls.

Examination of Crystal Uptake by LY—Whole blood cells treated with 1 mg/ml MSU or MPU were co-incubated with 20 μg/ml LY. LY is a membrane-impermeable fluorescent dye that is co-ingested when cells engulf targets (12). After 3 h, noningested MSU crystals were solubilized, and cells were analyzed by flow cytometry. MPU-containing phagocytes were analyzed after 1 h by flow cytometry and polarization microscopy.

Measurement of Intracellular Sodium Concentration—The relative intracellular sodium concentration was detected by Sodium Green, a fluorescent dye that changes its emission spectrum after binding of free sodium (13). Peripheral blood mononuclear cells were loaded with 10 μM Sodium Green for 30 min. Cells were resuspended in autologous plasma and incubated with 200 μg/ml MSU crystals at 37 °C for 2 h. After lysis of the crystals the intracellular sodium concentration was analyzed by cytofluorometry.

Determination of Cytokine Production in Vitro—Eighteen hours following MSU or MPU addition to whole blood cells, human IL-1β, IL-6, and TNFα production in culture supernatants was analyzed by multiplex bead technology and quantified by cytofluorometry. In cases indicated the cells were additionally treated with low doses of phorbol myristate acetate (6.25 ng/ml).

Cytokine Measurement after Acidic Treatment of MSU Crystals—Whole blood cells were incubated with 1 mg/ml MSU (pH 7.2) or MSU (pH 4.5) for 18 h. The IL-1β and IL-6 production in culture supernatants was analyzed as described above.

IL-1β Measurement after Inhibition of Lysosomal Acidification in Vitro—Whole blood cells were treated with 1 mg/ml MSU crystals for 30 min. After lysis of erythrocytes and of free MSU crystals, cells were resuspended in autologous plasma and incubated with inhibitors of lysosomal acidification (20 μM CQ, 10 mM NH_4Cl) and of aquaporins (30 μM $HgCl_2$, 50 μM phloretin), respectively, for 18 h (14, 15). IL-1β in culture supernatants was quantified as described previously.

IL-1β Measurement after Inhibition of Lysosomal Acidification in Vivo—Mice were anesthetized by inhalation of anesthesia, and 3 ml of sterile air was injected subcutaneously into the back to form an air pouch. Three days after the first injection, additional 2 ml of sterile air was injected into the pouch. CQ (10 mg/kg body weight) was injected intraperitoneally for 8 days. At the day of the last CQ injection 4 mg of MSU crystals in PBS or PBS as control were injected into the air pouches. Six hours later the pouch fluid was harvested, and IL-1β was determined by ELISA.

Analyses of Count and Composition of Infiltrating Cells into Air Pouch after CQ Treatment—Air pouches and CQ treatment of mice were performed as described above. Six hours after MSU treatment the pouch fluid was harvested, and cells were numbered by a Neubauer counting chamber and incubated with anti-CD11b antibody for 1 h. The percentage of $CD11b^+$ phagocytes was analyzed by flow cytometry.

Measurement of Human ProIL-1β and Caspase-1 Levels—Isolated untouched monocytes were treated with 200 μg/ml MSU crystals and incubated with inhibitors of lysosome acidification (20 μM CQ, 10 mM NH_4Cl) or of aquaporins (30 μM $HgCl_2$, 50 μM phloretin). The expression of proIL-1β and caspase-1 was analyzed 18 h after the treatments with an anti-proIL-1β antibody and anti-caspase-1 antibody by immuno-

blotting using standard protocols. Blots stained with Coomassie Blue dye serve as loading controls.

Measurement of Murine ProIL-1β and Caspase-1 levels—Air pouches and CQ treatment of mice were performed as described above. The expression of murine proIL-1β and caspase-1 was analyzed with an anti-proIL-1β antibody and anti-caspase-1 antibody by immunoblotting using standard protocols. Blots stained with Coomassie Blue dye served as loading controls.

Determination of ProIL-1β mRNA Level—The detection of human and mouse IL-1β mRNA levels was performed by quantitative RT-PCR analysis with an ABI Prism 7000 Sequence Detection System (Applied Biosystems) and qPCR Mastermix (Fermentas). Total RNA was extracted from isolated untouched monocytes or air pouch immigrating cells using TRIzol reagent (Invitrogen) according to the manufacturer's instructions. 1 μg of total RNA was subjected to DNase I treatment (Fermentas) and subsequently reversely transcribed with 200 units of RevertAid reverse transcriptase (Fermentas) in the presence of 50 μM random hexamers (GE Healthcare), 400 μM dNTPs (Fermentas), and 1.6 units/μl Ribolock RNase Inhibitor (Fermentas) in a final volume of 25 μl. 80 ng of the resulting cDNA was applied to the following quantitative RT-PCR analyses (20 μl final volume) with 50 nM primers and 100 nM probe for 18 S rRNA or 300 nM primers for human and mouse IL-1β and amplified with the standard temperature profile (2 min 50 °C, 10 min 95 °C, 40× (15 s 95 °C, 1 min 60 °C)). The following primers (Sigma) were used: human/mouse 18 S forward, CGGCTACCACATCCAAGGAA; human/mouse 18 S reverse, AGCTGGAATTACCGCGGC; human/mouse 18 S probe, Vic-TGCTGGCACCAGACTTGCCCTCC-Tamra; human IL-1β forward, CCTGAGCTCGCCAGTGAAAT; human IL-1β reverse, TTTAGGGCCATCAGCTTCAAAG; mouse IL-1β forward, TGACAGTGATGAGAATGACCTGTTC; mouse IL-1β reverse, AGGTTTGGAAGCAGCCCTTC. Relative quantification was performed employing the standard curve method. The results were normalized on 18 S rRNA, and the untreated cell population was used as calibrator.

Knockdown of AQP with siRNA Oligonucleotides—Transfection of THP-1 monocytes with *stealth*™ siRNA oligonucleotides (Invitrogen) targeting different AQPs was carried out twice (at day 0 and day 3) with the Gene Pulser II$^+$ Capacity Extender II (Bio-Rad) and 0.4-cm gap cuvettes. 5×10^6 THP-1 cells were electroporated with two different siRNA oligonucleotides/AQP (1 μM each) in 500 μl of Opti-MEM™ (Invitrogen) by a single pulse (800 microfarads, 200 V, time constant 20–30 ms). The cells were cultured for 3 days before electroporation was repeated. Stimulation with MSU crystals was carried out at day 6. Briefly, 200,000 THP-1 monocytes were incubated with 500 μg/ml MSU in 500 μl of RPMI 1640 medium + 10% FCS for 24 h. Cell-free culture supernatants were harvested, and IL-1β was measured by ELISA.

Analysis of MSU-induced IL-1β in Hypertonic Medium—Whole blood cells were incubated with 1 mg/ml MSU for 1 h. Then cells were exposed to extracellular hypertonicity (increased Na^+ or K^+). After 1 h, the cell swelling was analyzed by flow cytometry. The IL-1β and TNFα production in culture supernatants was measured after 18 h as described previously.

Morphological and Chemical Analyse of Urate Crystals by Scanning Electron (SEM-EDX) and Polarization Microscopy—Urate crystals were taken up in ethanol and dried on an aluminum/copper slide for S.E. analysis by Philips CM 30 T/STEM. The chemical composition of crystals was determined by an EDX detector. The crystals were analyzed by a Zeiss Axiovert 25 microscope equipped with polarizing filters.

Lysis of Erythrocytes/Crystals and Flow Cytometry—In whole blood assays the erythrocytes were automatically lysed by TQprep work station (Beckman Coulter) before measurement with an EPICS cytofluorometer. The data were analyzed with the System II software, version 3.0 (Coulter). Electronic compensation was used to eliminate bleed-through fluorescence. The lysis process also solubilized non-ingested MSU crystals.

RESULTS

The ingestion by blood-borne phagocytes of MSU crystals can be monitored by flow cytometry. During phagocytosis cells substantially increased their side scatter, reflecting increased "granularity" (Fig. 1*a*), whereas the size of the cell bodies (reflected by forward scatter) is virtually constant. However, some few minutes after the uptake of the crystals the cells start to swell as shown in the video sequence (Fig. 1*b*). The co-ingestion with MSU of LY, a membrane-impermeable fluorescent dye, confirmed the internalization of the crystals and excluded that they are merely attached to the cell surfaces (Fig. 1*c*). The plasma membranes of most cells remained ion-selective as demonstrated by the exclusion of propidium iodide (Fig. 1*d*). After *ex vivo* phagocytosis of MSU crystals by monocytes, IL-1β production is initiated. The importance of sodium in this process is substantiated by the inability to induce IL-1β of MPU crystals (Fig. 1*e*) even though they were readily ingested by phagocytes (supplemental Fig. 1).

After ingestion, the sodium-containing needle-shaped MSU crystals (Fig. 2, *a*, *c*, and *e*) localize in endocytotic vesicles that fuse with acidic lysosomes. The activity of proton pumps leads to a drop of the phagolysosomal pH. Under these conditions (*e.g.* pH below 5), sodium gets released from MSU crystals which consequently transform into diamond- or barrel-shaped crystals as shown by polarized light microscopy (Fig. 2*b*) and scanning electron microscopy (Fig. 2*d*). Loss of sodium from crystals exposed to acidic milieu was confirmed by laser-assisted energy-dispersive x-ray spectroscopy (Fig. 2*f*).

Furthermore, potassium is released after acidic treatment from MPU crystals, which also convert into barrel-shaped crystals (supplemental Fig. 2). In addition, acidic treatment of MSU crystals causes loss of activity for IL-1β secretion but not for the NALP3-independent cytokine IL-6 (supplemental Fig. 3).

Next, we analyzed whether sodium was also released when MSU crystals enter the endolysosomal compartment of living cells. For this purpose we loaded human blood monocytes with Sodium Green, enabling fluorescence-based quantification of intracellular sodium concentrations $[Na^+]_i$, and incubated them with and without MSU crystals. Cells without

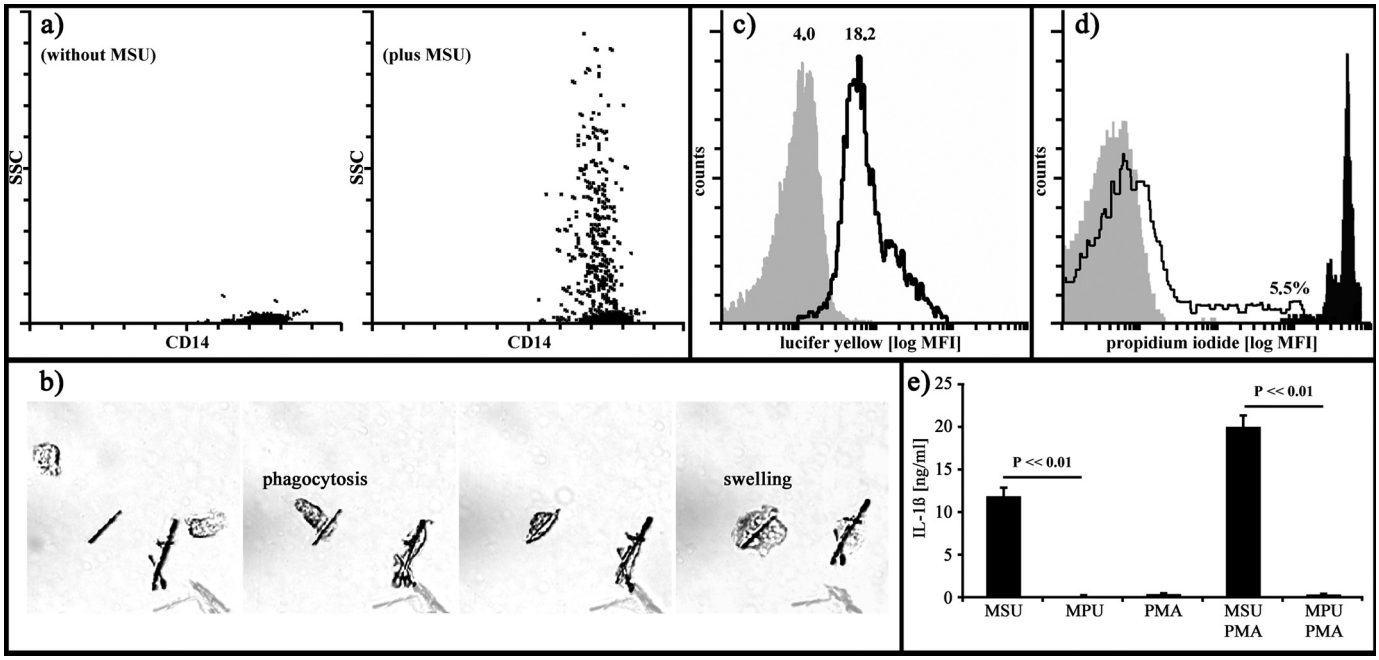

FIGURE 1. **Phagocytes swell and produce IL-1β after uptake of MSU crystals.** *a*, monocytes increase side scatter after phagocytosis of MSU. Whole blood was incubated with anti-CD14-PE in the absence (*left*) or presence (*right*) of MSU crystals (1 mg/ml) for 1 h. After lysis of erythrocytes, the cells were analyzed by flow cytometry. *b*, phagocytes swell after uptake of MSU crystals. Isolated PMN were taken up in autologous plasma and incubated with 400 μg/ml MSU crystals. Time lapse microscopy was performed for a period of 30 min with magnification of $\times$20. *c*, PMNs co-ingest MSU crystals and LY. Whole blood was incubated with 1 mg/ml MSU and 20 μg/ml membrane-impermeable LY for 3 h. After lysis of erythrocytes the cells were analyzed by flow cytometry. The cells show a low LY signal without treatment (*filled gray curve*) and a high positive LY signal after the uptake of MSU crystals (*black line*) because LY is co-ingested during phagocytosis. *d*, plasma membrane of PMNs remains ion selective after MSU uptake. Whole blood was incubated with 1 mg/ml MSU for 3 h; after lysis of erythrocytes PI (0.5 μg/ml) was added, and PI exclusion was measured by flow cytometry. Most PMNs that had been incubated in the presence and absence of MSU (*black line* and *filled gray curve*, respectively) maintained their membrane integrity. The *filled black curve* shows control PMNs that had been necrotized by heat treatment at 56 °C for 30 min. *e*, sodium (MSU) but not potassium (MPU) containing urate crystals induce IL-1β. Whole blood was incubated with 1 mg/ml MSU or MPU for 18 h. We prestimulated cells with a low concentration of phorbol myristate acetate (*PMA*) (6.25 ng/ml) if indicated. Only MSU is able to induce an IL-1β response, and there is also a cooperative effect with low phorbol myristate acetate.

MSU incubation showed a constant morphology (Fig. 2*g*), whereas MSU-treated cells immediately observed an increase in the granularity of the phagocytes reflecting uptake of the crystals (Fig. 2*h*). During this early phase MSU crystals are supposed to be predominantly within endocytotic vesicles. In phagocytes with increased granularity indicating recent ingestion of MSU crystals, the $[Na^+]_i$ was only marginally increased (Fig. 2*i*). In the period following the MSU ingestion, phagocytes were swelling as indicated by increased forward scatter and displayed markedly increased $[Na^+]_i$ content (Fig. 2*j*). We hypothesized that this sodium overload may cause transient hyperosmolarity of the cytoplasm, which is balanced by an aquaporin-mediated passive water influx concomitantly leading to a drop of $[K^+]_i$ and to assembly and activation of NALP3 inflammasomes.

To test this hypothesis we performed video microscopy and measured the release of IL-1β induced by MSU crystals in the presence of inhibitors of lysosome acidification and of aquaporins *in vitro*. As shown in supplementary Video 1, cells start to swell some minutes after ingestion of MSU crystals. Furthermore, the inhibitors of lysosome acidification (NH_4Cl) and of aquaporins ($HgCl_2$, phloretin) abrogated the induction of IL-1β, indicating that MSU-mediated IL-1β production depends on lysosome acidification and aquaporin-mediated passive water influx (16–18). The pharmaceutical inhibitor of lysosomal acidification, CQ, which is established as a drug for the treatment of autoimmune inflammatory diseases, also significantly reduced the IL-1β production by MSU crystals *in vitro* (Fig. 3*a*). Interestingly, these inhibitors did not decrease the IL-1β production as consequence of extracellular ATP, an established activator of potassium ion channels (supplemental Fig. 4). Furthermore, the inhibitors decreased swelling of phagocytes after MSU treatment (data not shown). Moreover, the proIL-1β and caspase-1 levels were not affected by the inhibitors of lysosomal acidification and of aquaporins (supplemental Fig. 5). The inhibitors only marginally influenced the IL-1β mRNA expression (data not shown). Analyzing the AQP profiles in THP-1 cells and primary human monocytes, we detected (<32 cycles) AQP0, AQP1, AQP3, and AQP11 in THP-1 cells and AQP9, in primary monocytes (supplemental Fig. 6*a*). Because AQP11 is not involved in water influx we down-regulated the expression of AQP0, AQP1, AQP3, and AQP9 in THP-1 cells. Interestingly, the down-regulation of a specific AQP resulted in the compensatory up-regulation of other AQPs (supplemental Fig. 6*b*). Still, the down-regulation of AQP0, AQP1, and AQP9 in THP-1 cells resulted in decreased IL-1β secretion (supplemental Fig. 6*c*). In contrast, the knockdown of AQP3 resulted in a increased IL-1β secretion by a strong compensatory up-regulation of AQP9 (data not shown). Increased extracellular hypertonicity prevents the effect of MSU on cell swelling and IL-1β secretion but not on TNFα production (supplemental Fig. 7).

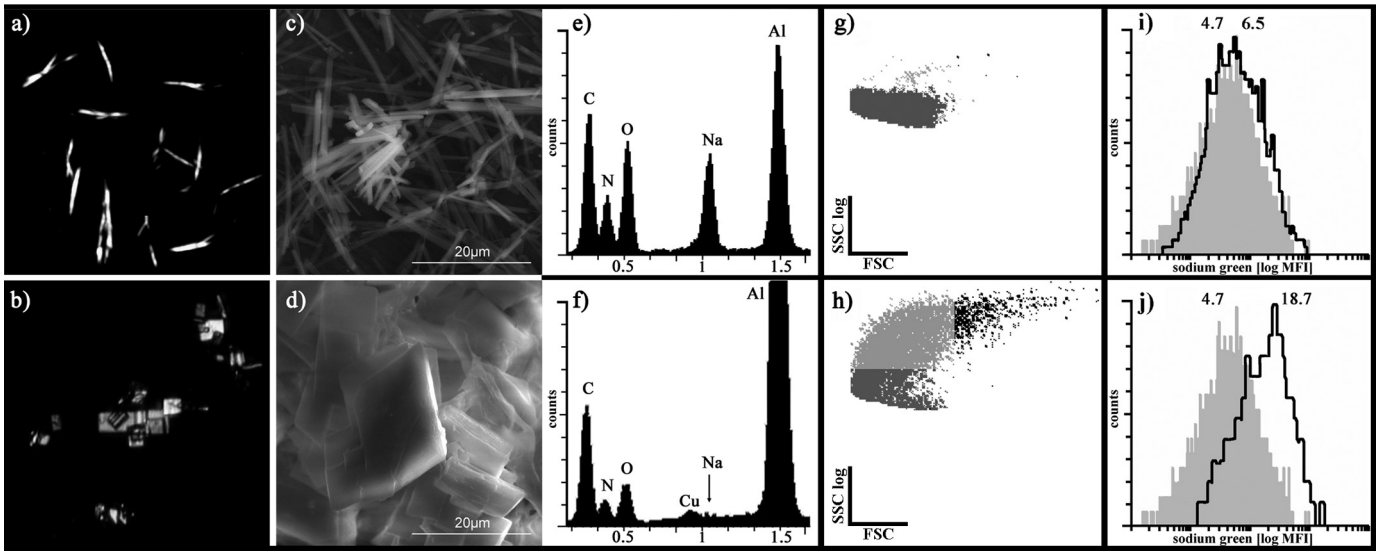

FIGURE 2. **Needle-shaped MSU crystals release sodium under acidic conditions.** *a*, *c*, and *e*, in sodium-rich fluids uric acid crystallizes as needle-shaped MSU crystals. A solution of 10 mM uric acid and 154 mM NaCl was adjusted to pH 7.2 and agitated for 3 days. The needle-shaped MSU crystals were stored in PBS (pH 7.0) and analyzed by polarization microscopy (*a*; ×40, composed picture). The MSU crystals were photographed by scanning electron microscopy (*c*, ×5000), and the elemental composition was analyzed by energy-dispersive x-ray spectroscopy (*e*). The spectrum of MSU crystals at pH 7.0 showed carbon, nitrogen, oxygen and sodium. *b*, *d*, and *f*, under acidic conditions MSU crystals release sodium and convert into barrel-shaped uric acid crystals. Needle-shaped MSU crystals in PBS (pH 7.0) were acidified to pH 4.5 with HCl. After 5 min, barrel-shaped crystals were identified by polarization microscopy and scanning electron microscopy (*b* and *d*). Crystals were analyzed as described in *a*, *c*, and *e*. The energy-dispersive x-ray spectrum of crystals at pH 4.5 showed only traces of residual sodium (*f*). MSU crystals were converted into uric acid crystals. Copper and aluminum are contaminants of the carrier plates. *g–j*, swollen monocytes contain markedly increased free sodium. Peripheral blood mononuclear cells were loaded with 10 μM cell-permeable Sodium Green, which allows measurement of intracellular free sodium ions. After washing, cells were incubated with 200 μg/ml MSU crystals for 3 h. After lysis of erythrocytes, cells were analyzed by flow cytometry. The morphology of the untreated (*g*) and MSU-treated cells (*h*) is shown here. MSU-treated cells that did not take up crystals are depicted in *dark gray* (*h*); these cells have a low sodium signal (*i*, *filled gray curve*, MFI 4.7). Note also that cells with only an increased side scatter after uptake of MSU (*h*, *light gray*) do not markedly change the sodium signal (*i*, *black line*, MFI 6.5). In swollen cells, reflected by a high forward scatter (*h*, *black*) intracellular free sodium ions were massively increased (*j*, *black line*, MFI: 18.7).

Next, we performed a murine *in vivo* study investigating the IL-1β induction of MSU crystals in the presence and absence of CQ. We generated air pouches and treated the mice intraperitoneally with CQ for 8 days. Then, MSU crystals or PBS as control were injected into the air pouches. Six hours later the pouch fluid was harvested, and IL-1β and IL-6 secretion was determined. In contrast to IL-6 secretion (data not shown), the IL-1β production was significantly reduced (Fig. 3*b*). The CQ treatment had no effect on the cell count and the composition of leukocytes infiltrating the air pouch (supplemental Fig. 8). Moreover, proIL-1β and caspase-1 levels were not affected by CQ in the murine air pouch model (supplemental Fig. 9). The IL-1β mRNA level was even increased by CQ treatment compared with untreated mice (data not shown).

In contrast to humans, most animals have functional urate oxidases that metabolize uric acid into allantoin, resulting in low baseline IL-1β responses to MSU. Nonetheless, the inhibition by CQ of lysosomal acidification significantly reduced the induction of IL-1β, supporting the mechanism of sodium overload and water influx being causative for NALP3 activation by MSU crystals.

DISCUSSION

It is well established that the activation of IL-1β and IL-18 is a three-step process, which requires transcriptional induction of the pro-proteins by Toll-like receptor signals, proteolytic maturation governed by caspase-1, as well as secretion into the extracellular space (19). There are also several pathways including caspase-1-independent ones leading to maturation/secretion of IL-1/IL-18 in which the inflammasomes play a central role (20, 21). In the case of NALP3 inflammasome, all decrypted activation pathways include low intracellular potassium as a common denominator. The drop of potassium is usually caused by escape through potassium pores or channels. Many bacterial toxins are pore-forming proteins that destroy the ion selectivity of cytoplasmic membranes (22). In addition, there are autologous receptor-activated ion channels like the ATP-responsive P2X7 (23). The importance of potassium in the process of inflammasome activation was highlighted by the fact that extracellular potassium abrogated the IL-1β activation by the inflammasome. This was also the case for MSU crystals. It was speculated that the latter may cause a MaxiK-mediated potassium efflux. However, the MaxiK inhibitor paxilline did not inhibit caspase-1 activation (8). Extracellular potassium not only inhibits potassium efflux from cells that have lost their ion selectivity but also converts MSU into inactive potassium urate crystals.

Based on our data we propose the following model for inflammasome activation after phagocytosis of MSU: (i) Monocytes take up crystals into endosomes. (ii) The fusion with acidic lysosomes of the endosomes leads to a drop in the pH (Fig. 4, *step 1*). (iii) The low pH causes the release of sodium from MSU crystals, which are converted into uric acid. (iv) The increase of $[Na^+]_i$ accounts for a rise of the intracellular

osmolarity (Fig. 4, *step 2*). (v) The increased sodium ion load of the cells is then passively balanced by water influx through aquaporins reflected by cellular swelling (Fig. 4, *steps 3* and *4*).

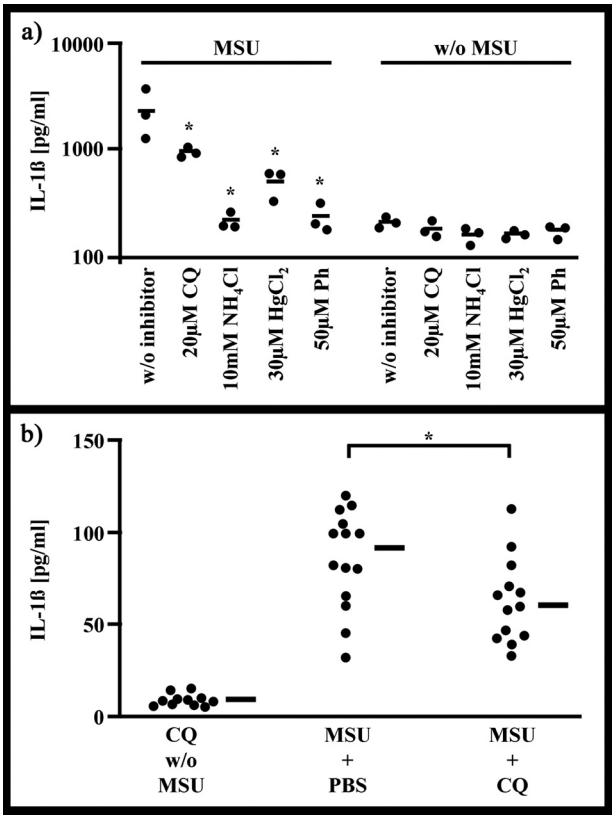

FIGURE 3. **Inhibitors of lysosome acidification and of aquaporins reduce the induction by MSU of IL-1β.** *a*, *in vitro*. Whole blood was incubated with 1 mg/ml MSU crystals for 30 min. Noningested crystals were lysed, and the cells were incubated with inhibitors of lysosome acidification (CQ, NH_4Cl) or of aquaporins ($HgCl_2$, phloretin (*Ph*)). After 18 h the IL-1β production was quantified in supernatants. Cultures without MSU served as controls (*bars*, mean). All inhibitors of lysosome acidification and of aquaporins significantly reduced the induction of IL-1β. *b*, *in vivo*. Air pouches were established in C57/BL6 mice (day −5). On days −7 to 0 the mice were intraperitoneally injected with 220 μg of the inhibitor of lysosome acidification CQ in PBS or with PBS alone. On day 0 MSU (4 mg in PBS) was injected into the air pouch if indicated. Six hours later the pouch fluid was harvested, and IL-1β was determined by ELISA. Mice without MSU served as control (*bars*, median). CQ significantly reduced the induction of IL-1β. Each *dot* represents one mouse.

(vi) The volume gain by water influx causes a drop in $[K^+]_i$ below the threshold and activates the NALP3 inflammasome (Fig. 4, *steps 4* and *5*).

Our model does not depend on potassium efflux. Instead it proposes a volume gain, which dilutes intracellular potassium concentrations. Hence, this physicochemical mechanism may account for the acute inflammation caused by one of the most common forms of arthritis in humans.

Our model of NALP3 activation by sodium overload succeeded by water influx is supported by acidic treatment of MSU crystals. The experimental loss of sodium from the crystals caused by the extracellular acidification renders an intracellular sodium release from the crystal impossible and abrogates IL-1β maturation. At the same time, the induction of the NALP3-independent cytokine IL-6 is not affected.

The down-regulation of candidate AQP also inhibits IL-1β production after MSU uptake. Water influx is delayed, and the intracellular drop of potassium is too small to activate the NALP3 inflammasome. Extracellular hypertonicity avoids cell swelling and IL-1β secretion. On the other hand it does not affect the expression of the NALP3 independent cytokine TNFα.

The reduction of the MSU-induced inflammation by inhibitors of lysosomal acidification and of aquaporins *in vitro* was confirmed *in vivo* by the use of the anti-inflammatory drug CQ. After treatment with this drug, the inflammatory response of air pouch cells to MSU crystals was ameliorated, although the amount and composition of infiltrating cells into the air pouch are similar to untreated mice. CQ treatment did not influence proIL-1β and caspase-1 levels of the air pouch cells. This shows that CQ specifically inhibited the conversion step of proIL-1β to the mature bioactive cytokine IL-1β.

The decreased IL-1β response to MSU after CQ treatment is of particular interest because the presence of urate oxidase in mice (but not in humans) efficiently hampers the MSU-related inflammation. Urate oxidase metabolizes the proinflammatory insoluble uric acid into the soluble allantoin (24). We therefore may expect an even higher

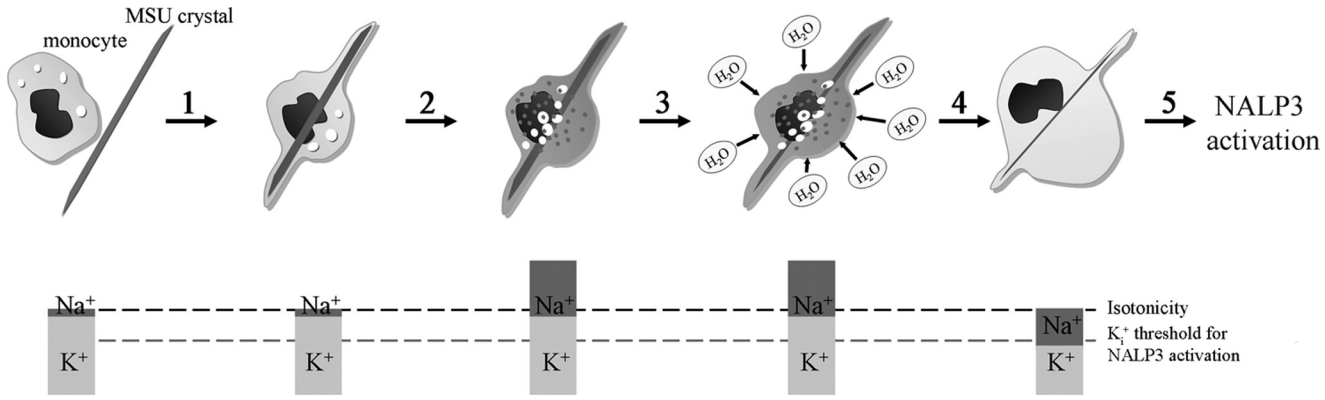

FIGURE 4. **Model of inflammasome activation by sodium overload and water influx.** Monocytes take up crystals into endosomes (*step 1*). The fusion with acidic lysosomes of the endosomes causes the release of sodium from the MSU crystal (*step 2*). The increase of $[Na^+]_i$ accounts for a rise of the intracellular osmolarity. The increased sodium ion load of the cells is then passively balanced by water influx through aquaporins (*step 3*). The volume gain leading to cellular swelling causes a drop in $[K^+]_i$ below the threshold required for NALP3 inflammasome activation (*steps 4* and *5*).

efficacy of CQ in humans, which could be of relevance in the treatment of gout.

In conclusion, we provide evidence for a mechanism of how MSU crystals induce the NALP3 inflammasome and trigger inflammation. Uptake of MSU, liberation of huge amounts of sodium, transient hyperosmolarity, and water influx dilute intracellular potassium concentration and, thereby, activate IL-1β maturation.

Acknowledgment—We thank Falk Nimmerjahn for the critical reading of the manuscript.

REFERENCES

1. Roddy, E., Zhang, W., and Doherty, M. (2007) *Ann. Rheum. Dis.* **66,** 1374–1377
2. Celsus, A. C., Scheller, E., and Frieboes, W. (1906) *Aulus Cornelius Celsus über die Arzneiwissenschaft in acht Büchern*, F. Vieweg und Sohn, Braunschweig, Germany
3. Martinon, F., and Glimcher, L. H. (2006) *J. Clin. Invest.* **116,** 2073–2075
4. Shi, Y., Evans, J. E., and Rock, K. L. (2003) *Nature* **425,** 516–521
5. Martinon, F., Pétrilli, V., Mayor, A., Tardivel, A., and Tschopp, J. (2006) *Nature* **440,** 237–241
6. Lamkanfi, M., and Dixit, V. M. (2009) *Immunol. Rev.* **227,** 95–105
7. Pétrilli, V., Dostert, C., Muruve, D. A., and Tschopp, J. (2007) *Curr. Opin. Immunol.* **19,** 615–622
8. Pétrilli, V., Papin, S., Dostert, C., Mayor, A., Martinon, F., and Tschopp, J. (2007) *Cell Death Differ.* **14,** 1583–1589
9. Nilsson, C., Aboud, S., Karlén, K., Hejdeman, B., Urassa, W., and Biberfeld, G. (2008) *Clin. Vaccine Immunol.* **15,** 585–589
10. Schorn, C., Janko, C., Munoz, L., Schulze, C., Strysio, M., Schett, G., and Herrmann, M. (2009) *Autoimmunity* **42,** 314–316
11. Peng, L., Jiang, H., and Bradley, C. (2001) *Hua Xi Yi Ke Da Xue Xue Bao* **32,** 602–604, 620
12. Takeuchi, K., and Yoshii, K. (2008) *Chem. Senses* **33,** 425–432
13. Lo, C. J., Leake, M. C., and Berry, R. M. (2006) *Biophys. J.* **90,** 357–365
14. Furuchi, T., Aikawa, K., Arai, H., and Inoue, K. (1993) *J. Biol. Chem.* **268,** 27345–27348
15. Rogers, S. W., and Rechsteiner, M. (1988) *J. Biol. Chem.* **263,** 19843–19849
16. Misinzo, G., Delputte, P. L., and Nauwynck, H. J. (2008) *J. Virol.* **82,** 1128–1135
17. Bramley, H., Turner, N. C., Turner, D. W., and Tyerman, S. D. (2009) *Plant Physiol.* **150,** 348–364
18. Haddoub, R., Rützler, M., Robin, A., and Flitsch, S. L. (2009) *Handb. Exp. Pharmacol.* 385–402
19. Figueiredo, M. D., Vandenplas, M. L., Hurley, D. J., and Moore, J. N. (2009) *Vet. Immunol. Immunopathol.* **127,** 125–134
20. Dinarello, C. A. (2009) *Annu. Rev. Immunol.* **27,** 519–550
21. Okamoto, M., Liu, W., Luo, Y., Tanaka, A., Cai, X., Norris, D. A., Dinarello, C. A., and Fujita, M. (2010) *J. Biol. Chem.* **285,** 6477–6488
22. Kloft, N., Busch, T., Neukirch, C., Weis, S., Boukhallouk, F., Bobkiewicz, W., Cibis, I., Bhakdi, S., and Husmann, M. (2009) *Biochem. Biophys. Res. Commun.* **385,** 503–506
23. Colomar, A., Marty, V., Médina, C., Combe, C., Parnet, P., and Amédée, T. (2003) *J. Biol. Chem.* **278,** 30732–30740
24. Stamp, L. K., O'Donnell, J. L., and Chapman, P. T. (2007) *Intern. Med. J.* **37,** 258–266